

## Stress-induced birefringence in the isotropic phases of lyotropic mixtures

P. R. G. Fernandes,<sup>\*</sup> J. N. Maki, L. B. Gonçalves, B. F. de Oliveira, and H. Mukai

*Laboratório de Fluidos Complexos, Departamento de Física, Universidade Estadual de Maringá, Avenida Colombo 5790, 87020-900 Maringá, Paraná, Brazil*



(Received 20 November 2017; published 22 February 2018)

In this work, the frequency dependence of the known mechano-optical effect which occurs in the micellar isotropic phases ( $I$ ) of mixtures of potassium laurate (KL), decanol (DeOH), and water is investigated in the range from 200 mHz to 200 Hz. In order to fit the experimental data, a model of superimposed damped harmonic oscillators is proposed. In this phenomenological approach, the micelles (microscopic oscillators) interact very weakly with their neighbors. Due to shape anisotropy of the basic structures, each oscillator  $i$  ( $i = 1, 2, 3, \dots, N$ ) remains in its natural oscillatory rotational movement around its axes of symmetry with a frequency  $\omega_{0i}$ . The system will be in the resonance state when the frequency of the driving force  $\omega$  reaches a value near  $\omega_{0i}$ . This phenomenological approach shows excellent agreement with the experimental data. One can find  $f \sim 2.5, 9.0$ , and 4.0 Hz as fundamental frequencies of the micellar isotropic phases  $I$ ,  $I_1$ , and  $I_2$ , respectively. The different micellar isotropic phases  $I$ ,  $I_1$ , and  $I_2$  that we find in the phase diagram of the KL-DeOH-water mixture are a consequence of possible differences in the intermicellar correlation lengths. This work reinforces the possibilities of technological applications of these phases in devices such as mechanical vibration sensors.

DOI: [10.1103/PhysRevE.97.022705](https://doi.org/10.1103/PhysRevE.97.022705)

### I. INTRODUCTION

Lyotropic liquid crystals (LLCs) are interesting materials formed by the mixture of amphiphilic molecules in a solvent at a given temperature and relative concentrations [1]. From the critical micellar concentration the amphiphilic molecules self-assemble spontaneously into molecular aggregates known as micelles [2,3]. The existence of the shape anisotropy of these basic constituents (micelles) is a fundamental characteristic of LLCs. The mixture composed of potassium laurate (KL), decanol (DeOH), and water shows a rich phase diagram [4] with nematic phases surrounded by micellar isotropic phases ( $I$ ) [5,6]. Usually, in the literature, isotropic phases of lyotropic mixtures do not arouse as much interest as their nematic phases. However, in the isotropic phases of lyotropic mixtures, an interesting phenomenon, well known as flow-induced birefringence, occurs [7–10]. This phenomenon has also been observed in the isotropic phase of thermotropic liquid crystals [11–15] and sponge phases [16]. Recently, the shear-induced optical effect in the isotropic phases of liquid crystals has been reviewed and the elastomeric behavior of the isotropic phases has been reported [17]. In the case of isotropic phases of the KL-DeOH-water mixture, as described in Refs. [8,9], the flow is produced by the falling movement of a flat plate inside the sample at the isotropic phase. With a polarized laser beam crossing through the sample parallel to the surface of the plate, the emergence light from the analyzer is detected. Another way of obtaining a similar induced birefringence effect is by subjecting the sample to external mechanical vibrations. The induced order by mechanical vibrations in the KL-DeOH-water mixture at the isotropic phase has been experimentally investigated and interpreted as a resonance effect

[18,19]. However, a phenomenological approach describing the frequency dependence of this interesting effect is lacking.

In the present work, our goal is to give a phenomenological interpretation of the stress-induced effect experimentally investigated in the low-frequency domain. The proposed approach considers the isotropic phases of the LLC as an elastic medium formed by damped harmonic oscillators. The micelles (microscopic oscillators) are connected by “springs” with the same elastic constant. The microscopic oscillators have a shape anisotropy and they are permanently in an oscillatory rotational movement with respect to their axes of symmetry. This approach showed excellent agreement with the experimental data for all isotropic phases of the ternary (KL-DeOH-water) mixtures investigated. The existence of resonance frequencies in these phases is a strong indication of the intrinsic oscillatory nature of micelles. In addition, this fact is further evidence of the hidden elasticity at the submillimeter length scale in the liquid state, as reported by Kahl *et al.* [20,21]. No phenomenological model has been proposed addressing the frequency dependence (200 mHz to 200 Hz) of this interesting effect that occurs in the isotropic phases of liquid crystals. Furthermore, our main finding is to show that the isotropic phases of liquid crystals have an oscillating microscopic nature that can resonate with external perturbations. From this work we highlight the strong possibilities of technological applications of these phases in devices such as mechanical vibration sensors [22,23].

### II. EXPERIMENT

#### A. Samples

The DeOH is from Sigma (p.a.>99%), the KL is synthesized and recrystallized in our laboratory from commercial

<sup>\*</sup>pricardo@dfi.uem.br

TABLE I. Composition of the samples studied. Here  $L_1$  and  $L_2$  are lamellar phases observed at low and high temperatures, respectively;  $I$ ,  $I_1$ , and  $I_2$  are isotropic phases; and  $N$  is the nematic phase.

Sample	KL (wt. %)	DeOH (wt. %)	Water (wt. %)	Molar ratio $C = \frac{[\text{KL}]}{[\text{DeOH}]} \text{ (mol \%)}$	Phase transitions	
					Temperatures ( $T_c$ )	
I	27.79	6.93	65.28	2.65	$L_1 \xrightarrow{T_c=8.8^\circ\text{C}} I \xrightarrow{T_c=47.0^\circ\text{C}} L_2$	
II	27.09	6.69	65.22	2.67	$L_1 \xrightarrow{T_c=12.0^\circ\text{C}} I \xrightarrow{T_c=51.0^\circ\text{C}} L_2$	
III	26.66	6.07	67.27	2.96	$I_1 \xrightarrow{T_c=22.8^\circ\text{C}} N \xrightarrow{T_c=44.6^\circ\text{C}} I_2$	

lauric acid (Sigma, p.a.>99%), and the deionized and distilled water is from a commercial deionizer (Quimis, Model 180M22). Mixtures are prepared, at room temperature ( $\sim 25^\circ\text{C}$ ), in previously well-cleaned glass tubes. Each compound of the mixture is carefully weighed at a 0.005% accuracy with the following steps: initially adding the desired amount of KL in the test tube, followed by DeOH addition and finally the water. The test tube is closed with its screw tap and sealed with parafilm to avoid changes in the relative concentration of the mixture due to evaporation. In order to ensure good homogenization, initially, the sample is homogenized by hand and afterward shaken in an electric vibrator and centrifuged for several minutes to eliminate any bubbles and foams formed. The process is repeated until the sample is thoroughly homogeneous. After that, the sample is kept at rest for a few hours before being used. Before starting the measurements, all investigated mixtures are in isotropic phase at room temperature, showing the effect of stress-induced birefringence. To verify the presence of this effect, the tube with the desired mixture inside is placed between crossed polarizers. When the tube is shaken, a strong stress-induced birefringence can be observed. A polarized light microscopy (PLM) technique (Microscope Leica, Model DM-LP) coupled to a CCD camera (DXC-107, Sony) is used to verify the phase transition temperatures of the samples (Table I). The sample temperature is controlled by a thermostatic circulating bath. By PLM technique, it is observed that samples I and II are in the isotropic phase  $I$  in a temperature range of  $\Delta T \sim 39.0^\circ\text{C}$ . Besides that, two isotropic-to-lamellar phase transitions [24] are observed in these lyotropic mixtures, one of them at low and the other at high temperatures. Table I shows the relative [KL] concentrations of each compound of the samples (in wt. %) and their molar ratios  $C = [\text{KL}]/[\text{DeOH}]$  with [KL] and [DeOH] in mol %. As pointed in Ref. [19],  $C$  values of samples I and II have been found in the range  $2.6 \leq C \leq 2.9$ . For  $C > 2.9$  (sample III), the mixture has a nematic phase between two isotropic phases. When the lamellar phases, denoted by  $L_1$  (at low temperatures) and  $L_2$  (at high temperatures), are reached their optical textures are characterized by the existence of bright spots on a dark background. The bright spots in  $L_1$  always show a higher optical contrast than those observed at high temperatures ( $L_2$ ). Sample III shows a nematic phase  $N$  surrounded by two isotropic phases, denoted by  $I_1$  and  $I_2$ , which are, respectively, isotropic phases below and above the  $N$  phase. When the samples are in the  $I$ ,  $I_1$ , or  $I_2$  phases their optical textures are totally dark, which is the typical texture of the isotropic phase.

**B. Experimental setup**

The experimental setup (see Fig. 1) is similar that used in Ref. [19]. The lyotropic mixture is encapsulated in a quartz container (Hellma) of rectangular section with dimensions  $a = b = 12.56 \text{ mm}$  and  $c = 45.0 \text{ mm}$  ( $a$ ,  $b$ , and  $c$  are parallel to the  $x$ ,  $z$ , and  $y$  axes, respectively). The cell is placed in a temperature-controlled device ( $0.1^\circ\text{C}$  stability). The  $y$  axis of the laboratory frame is parallel to the  $c$  dimension of the cell; the  $x$  axis is the laser beam (He-Ne, 10 mW,  $\lambda = 633 \text{ nm}$ ) direction. Aiming at obtaining the results of light transmittance, the sample, at the isotropic phase, is placed between cross polarizers oriented at  $45^\circ$  to the external mechanical perturbation direction. A thermostatic circulating bath (stability  $0.1^\circ\text{C}$ ) is used to control the temperature of the sample. The external force is applied to the cell (along the  $z$  axis) by means of a thin rod of aluminum (80 mm long and 1.6 mm wide). The thin rod is coupled to a loudspeaker (model EG 102 300W from ETM, Brazil) connected to a function generator (Stanford DS335). The external signal is a square wave with an amplitude of  $1.1V_{\text{rms}}$  and frequencies ranging from 200 mHz to 200 Hz. In this frequency range, the applied external voltage (from  $1.0V_{\text{rms}}$  to  $5.0V_{\text{rms}}$ ) has a linear behavior with respect to the strain amplitude produced by the loudspeaker. A Teflon tip at the end of the thin rod is used to avoid damages to the sample container. The thin rod touches the cell and promotes the movement of the sample. The entire experimental setup is on a pneumatic optical table (Newport RS2000) to avoid spurious mechanical vibrations. Beyond

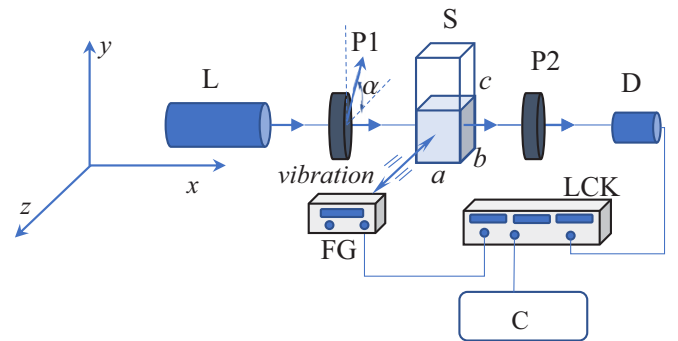


FIG. 1. Sketch of the setup used to measure sample transmittance as a function of frequency:  $a \parallel x$ ,  $b \parallel z$ ,  $c \parallel y$ , L is the light source, P1 and P2 are crossed polarizers,  $\alpha = 45^\circ$ , S is the sample; D is the photodiode, FG is the function generator, LCK is the lock-in, and C is the computer.

the analyzer, a photodiode (PIN 1623, New Focus) detects the light intensity that comes mainly from the stress-induced birefringence effect. The optical transmittance of the sample is measured in a rectangular window of the center of the Hellma cell and about 3 mm below of the air-sample interface. In order to minimize the signal fluctuations, a lock-in amplifier (Stanford SR830) is used.

### III. RESULTS AND DISCUSSION

The measurements of the optical transmittance induced by mechanical perturbations in the isotropic phase of a LLC are performed by using the samples and experimental setup described in Sec. II B. At first, the quadratic relationship between the amplitude of the applied external signal and optical transmittance of the sample is confirmed in the frequency range used (from 200 mHz to 200 Hz). After that, an amplitude of  $1.1V_{\text{rms}}$  for the external mechanical signal is chosen. All investigated isotropic phases are optically transparent and, as expected, their optical textures are completely dark when viewed between crossed polarizers. In these isotropic fluids, due to the well-known shape anisotropy of their basic structures (bricklike micelles) [1], it is possible to induce birefringence by velocity gradients or flows imposed on the sample. The time dependence of the flow-induced birefringence in the isotropic phases of lyotropic mixtures has been investigated and the scale of their relaxation process is between 5 and 25 ms [16]. However, it is also possible to induce birefringence by means of an applied external mechanical stress on the isotropic micellar solution. In this work we report a mechanically induced birefringence in the low-frequency range (0–35 Hz). In this work, a phenomenological model considering the micellar isotropic phases as formed by damped harmonic oscillators is proposed (see Sec. IV). Due to micellar shape anisotropy, each microscopic oscillator  $i$  ( $i = 1, 2, 3, \dots, N$ ) remains in its natural oscillatory rotational movement around its axes of symmetry with a frequency  $\omega_{0i}$ . The system will be in the resonance state when the frequency of the driving force  $\omega$  reaches a value near  $\omega_{0i}$ . Then when these fluids are submitted to a periodic external vibration along the  $z$  axis, the vector  $\vec{n}$  of each micelle that is naturally oscillating randomly will oscillate only around this preferential direction. The polarizer direction makes an angle  $\beta = 45^\circ$  with respect to the  $yz$  plane. In this way, each microscopic oscillator contributes to the total optical transmittance of the sample  $T(\omega)$  measured on the  $x$  axis.

Figures 2 and 3 show the maximum light transmittances of the isotropic phase  $I$  of samples I and II as a function of external mechanical frequencies at different temperatures. In Fig. 2, one sharp peak can be observed at the frequency  $f = (12.0 \pm 0.5)$  Hz. As expected, this resonance frequency has no concentration dependence on the relative concentrations of each sample. However, we note that only for sample I the number of normal modes increases with increasing temperature. Due to its proximity to the nematic phase [1,4], the highest optical transmittance is observed at  $T = 43.4^\circ\text{C}$ . In addition, isotropic phases  $I$  near the lamellar phase at high temperatures ( $L_2$ ) always show a higher number of resonant frequencies (at least four) than those found near the  $L_1$  phase (see Table II). On the other hand, sample III, with isotropic

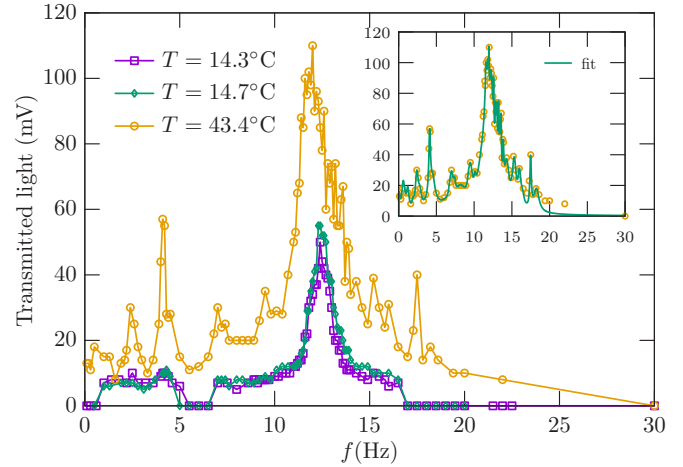


FIG. 2. Optical transmittance against frequency of the stress-induced birefringence in the isotropic phase of the KL-DeOH-water mixtures for sample I:  $L_1 \xrightarrow{T_c=8.8^\circ\text{C}} I \xrightarrow{T_c=47.0^\circ\text{C}} L_2$ . Continuum lines are only guides to the eye. The inset shows the optical transmittance of the stress-induced birefringence effect in the isotropic phase of sample I at  $T = 43.4^\circ\text{C}$ . The solid line is the fit of Eq. (3) by using  $N = 35$  damped harmonic oscillators. The fit values of the damping parameter are in the range  $0 < \gamma_i < 0.4$ .

phases  $I_1$  and  $I_2$  surrounded by a nematic phase  $N$ , always has a smaller number of resonance frequencies than those isotropic phases  $I$  surrounded by lamellar phases  $L_1$  and  $L_2$ . By taking the isotropic phases of the samples displayed in Table II, one can find  $f \sim 2.5, 9.0,$  and  $4.0$  Hz as fundamental frequencies of the micellar isotropic phases  $I, I_1,$  and  $I_2$ , respectively. We observed that at least one resonance frequency in the phase  $I_1$  and four of them in the isotropic phase  $I_2$  can be found. However, in isotropic phases  $I$  up to seven vibrational modes can be found. These resonance frequencies are expected to be a measurement of the normal modes of oscillations proper to a rectangular container. As known, at the resonance state the

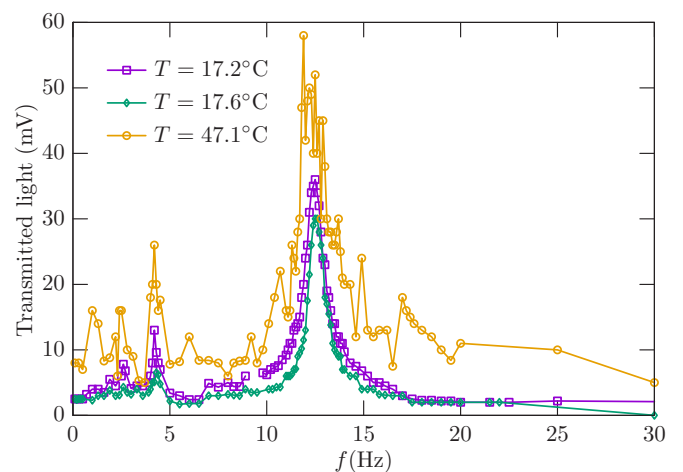


FIG. 3. Optical transmittance against frequency of the stress-induced birefringence in the isotropic phase of the KL-DeOH-water mixtures for sample II:  $L_1 \xrightarrow{T_c=12.0^\circ\text{C}} I \xrightarrow{T_c=51.0^\circ\text{C}} L_2$ . Continuum lines are only guides to the eye.

TABLE II. Resonance frequencies of the stress-induced birefringence of LLC mixtures at isotropic phases ( $I$ ,  $I_1$ , and  $I_2$ ).

Sample	Temperature (°C)	Resonance frequencies (Hz)					
I	14.3	2.5	4.2	7.0	12.4		
I	14.7	4.3		7.2	12.4		
I	43.4	2.4	4.1	7.0	9.5	12.0	15.2 17.5
II	17.2	2.6	4.2	7.0	12.5		
II	17.6	4.3		7.0	12.5		
II	47.1	2.5	4.2	6.0	9.5	11.9	17.0
III	18.0	9.0					
III	21.0	9.0					
III	21.5	9.0					
III	46.9	4.0	7.0	9.0	12.0		
III	48.5	4.0	7.0	9.0	12.0		

applied force and the velocity of microscopic oscillators are in phase and the rate of energy transfer from the applied force to the oscillators is maximum [23]. The existence of resonance frequencies in the isotropic phases of the KL-DeOH-water mixture is additional strong evidence of the elastic nature of the micellar solutions [25]. This fact strengthens the evidence of the hidden elasticity at the submillimeter length scale in the liquid state as recently reported by Kahl *et al.* [20]. The optical transmittance behavior as a function of frequency is similar as those obtained in Refs. [18,19]. However, in these references, resonance frequencies above 20 Hz have also been observed. We point out that one reason for this is due to the use of larger voltages of external signal ( $V_{\text{rms}} = 5.0$  V) than that used in this work ( $V_{\text{rms}} = 1.1$  V). Another one can be due to small probable differences in the mass of each molecular aggregate (micelle). Despite this, we have obtained good reproducibility of the optical spectrum of the mechano-optical effect for  $f < 20$  Hz.

The inset in Fig. 2 shows the experimental data of the optical transmittance (mV) of the stress-induced birefringence effect fitted with Eq. (3) containing  $N = 35$  superimposed damped harmonic oscillators. The fit values of the damping parameter are in the range  $0 < \gamma_i < 0.4$ . The fits were performed by using *Mathematica*<sup>®</sup> software with an iterative method. Our approach was applied only to experimental data of sample I at  $T = 43.4$  °C due to its highest transmitted light intensity. However, we note that this approach obtained excellence agreement with experimental results.

Figure 4 shows the total transmitted light against the external mechanical frequency of sample III (see Table I). This sample have a nematic phase surrounded by two isotropic phases: one at high temperature, denoted by  $I_2$ , and the other at low temperature, denoted by  $I_1$ . In both isotropic phases the stress-induced birefringence is clearly characterized by the existence of peaks in the optical transmittance. One can observe that in the isotropic phases at low temperatures ( $T < 22.8$  °C) there is only one vibrational mode ( $f = 9.0$  Hz), while at high temperatures ( $T > 44.6$  °C) we have found up to four resonance frequencies. However, the number of normal modes at the  $I_1$  and  $I_2$  phases is less than that found in the  $I$  phase (up to seven). The different micellar isotropic phases ( $I$ ,  $I_1$ , and  $I_2$ ) that have been found by us in the phase diagram of the KL-DeOH-water mixture are the consequence

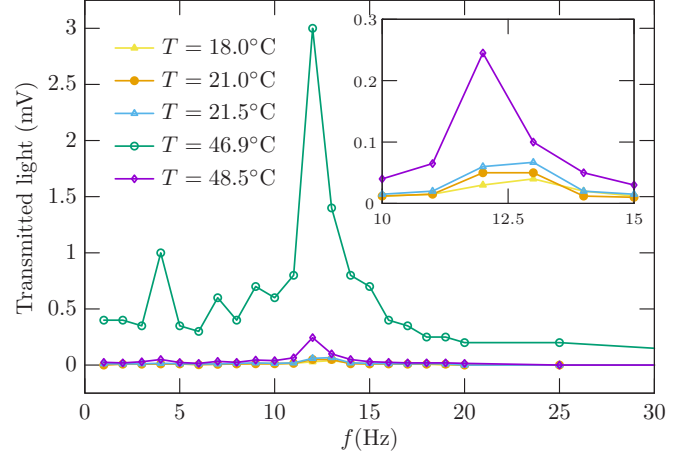


FIG. 4. Optical transmittance against frequency of the stress-induced birefringence in the isotropic phase of the KL-DeOH-water mixtures for sample III:  $I_1 \xrightarrow{T_c=22.8^\circ\text{C}} N \xrightarrow{T_c=44.6^\circ\text{C}} I_2$ . Continuum lines are only guides to the eye. The inset shows a close-up around the sharp peak.

of possible differences in the intermicellar correlations length ( $l \sim 10^{-4}$  cm [16]).

#### IV. PHENOMENOLOGICAL MODEL

In order to fit our experimental results, we are proposing a phenomenological model considering the micellar isotropic phases as formed by damped harmonic oscillators. In this phenomenological approach, due to micellar shape anisotropy (orthorhombic micelles) [1], the oscillators (micelles) are permanently in an oscillatory rotational movement around their axes of symmetry. It is assumed that each harmonic oscillator  $i$  ( $i = 1, 2, 3, \dots, N$ ), with mass  $m_i$ , has natural frequency  $\omega_{0i}$ . In this approach we are considering that the displacement of the micelle is expressed by the coordinate  $\theta_i$  and the damping term  $\gamma_i$  due to fluid viscosity has a linear relationship with velocity. By considering an external oscillating applied force with amplitude  $F_{0i}$ , phase  $\delta$ , and angular frequency  $\omega = 2\pi f$  (with  $f$  expressed in hertz), the one-dimensional dynamic equation of the proposed mechanical model can be written as [25,26]

$$\frac{d^2}{dt^2}\theta_i(t) + \gamma_i \frac{d}{dt}\theta_i(t) + \omega_{0i}\theta_i(t) = \frac{F_{0i}}{m_i} \sin(\omega t + \delta). \quad (1)$$

When the frequency of the driving force  $\omega$  reaches a value near the undamped natural frequency of the  $i$  oscillator without damped  $\omega_{0i}$ , each independent oscillator of the sample will be in the resonance state. In this specific state, the applied force and the velocity of microscopic oscillators (micelles) are in phase and the rate of energy transfer from the applied force to the oscillators is maximum. However, as we known [26,27], in the resonance regime the average value of the rate of change of energy  $\frac{d\langle E \rangle}{dt}$  in a period is null. This implies that the average power supplied by the external force is equal to the average power dissipated due to system damping [27]. In this way, the average power  $\langle P_i \rangle$  transferred to each  $i$  oscillator can be



expressed by

$$\langle P_i(\omega) \rangle = \frac{\gamma_i \omega^2 F_{0i}^2}{2m_i [(\omega_{0i}^2 - \omega^2)^2 + \gamma_i^2 \omega^2]}. \quad (2)$$

In the resonance state ( $\omega = \omega_{0i}$ ), the optical transmittance intensity  $I_i(\omega)$  will be maximum due to the maximum orientational alignment reached by each micelle of the solution. The total optical transmittance of the sample  $T(\omega)$  can be expressed by the superposition of the individual intensities  $I_i$  associated with each one of the harmonic oscillators in the steady state as

$$T(\omega) = I_1(\omega) + I_2(\omega) + I_3(\omega) + \dots + I_N(\omega), \quad (3)$$

where  $I_i(\omega) = \langle P_i(\omega) \rangle / A$  and  $A$  is the area of the section illuminated by the laser beam.

## V. CONCLUSION

In this work, we investigated the effect of stress-induced birefringence that occurs in isotropic phases of KL-DeOH-water mixtures. In order to fit a frequency dependence of the optical transmittance of this effect, a damped harmonic oscillator approach was proposed. One could find  $f \sim 2.5, 9.0$ , and  $4.0$  Hz as fundamental frequencies of the micellar isotropic phases  $I$ ,  $I_1$ , and  $I_2$ , respectively. We observed that there is at least one vibrational mode at the phase  $I_1$  and four of them at the isotropic phase  $I_2$ . However, at isotropic phases  $I$  between

two lamellar phases (samples I and II), up to seven vibrational modes can be found. These resonance frequencies are expected to be a measurement of the normal vibration modes proper to a rectangular container. The proposed phenomenological model considering the micellar isotropic phases as formed by damped harmonic oscillators has obtained excellent agreement with the experimental data. We noticed that differences in the intermicellar correlation lengths in the isotropic phases can produce the different micellar isotropic phases  $I$ ,  $I_1$ , and  $I_2$  of the KL-DeOH-water mixture. From this work we highlight the strong possibility of technological applications of these phases in devices such as mechanical vibration sensors. Furthermore, the existence of resonance frequencies in the isotropic phases of the KL-DeOH-water mixture strongly illustrates the oscillatory nature of its microscopic basic structures (micelles) in these phases.

## ACKNOWLEDGMENTS

The authors thank the National Council for Scientific and Technological Development (CNPq Grant No. 465259/2014-6), the Coordination for the Improvement of Higher Education Personnel (CAPES), the National Institute of Science and Technology Complex Fluids (INCT-FCx), the São Paulo Research Foundation (FAPESP Grant No. 2014/50983-3), and the Paraná Research Foundation (Fundação Araucária Grant No. 2017/47223), from Brazil, for financial support.

- 
- [1] A. M. Figueiredo Neto and S. Salinas, *The Physics of Lyotropic Liquid Crystals: Phase Transitions and Structural Properties* (Oxford University Press, Oxford, 2005).
- [2] C. Tanford, *The Hydrophobic Effect: Formation of Micelles and Biological Membranes* (Wiley-Interscience, New York, 1980).
- [3] G. Burducea, Rom. Rep. Phys. **56**, 66 (2004).
- [4] L. J. Yu and A. Saupe, *Phys. Rev. Lett.* **45**, 1000 (1980).
- [5] A. M. Figueiredo Neto, L. Liebert, and Y. Galerne, *J. Phys. Chem.* **89**, 3737 (1985).
- [6] V. V. Berejnov, V. Cabuil, R. Perzynski, Y. L. Raikher, S. N. Lysenko, and V. N. Sdobnov, *Crystallogr. Rep.* **45**, 493 (2000).
- [7] J. P. Decruppe, R. Cressely, R. Makhlofi, and E. Cappelaere, *Colloid. Polym. Sci.* **273**, 346 (1995).
- [8] P. R. G. Fernandes and A. M. Figueiredo Neto, *Phys. Rev. E* **51**, 567 (1995).
- [9] P. R. G. Fernandes and A. M. Figueiredo Neto, *Phys. Rev. E* **56**, 6185 (1997).
- [10] M. Simões, P. R. Fernandes, A. J. Palangana, and S. M. Domiciano, *Phys. Rev. E* **64**, 021707 (2001).
- [11] T. W. Stinson and J. D. Litster, *Phys. Rev. Lett.* **25**, 503 (1970).
- [12] P. Martinoty, S. Candau, and F. Debeauvais, *Phys. Rev. Lett.* **27**, 1123 (1971).
- [13] A. D. Rey and M. M. Denn, *Mol. Cryst. Liq. Cryst.* **153**, 301 (1987).
- [14] A. D. Rey and M. M. Denn, *Liq. Cryst.* **4**, 253 (1989).
- [15] L. M. Sabirov and D. I. Semenov, *Opt. Spectrosc.* **101**, 299 (2006).
- [16] G. Porte, J. Appell, P. Bassereau, and J. Marignan, *J. Phys. (Paris)* **50**, 1335 (1989).
- [17] P. Kahl and L. Noirez, *Liq. Cryst. Rev.* **4**, 135 (2016).
- [18] D. A. de Oliveira and P. R. Fernandes, *Braz. J. Phys.* **32**, 531 (2002).
- [19] P. R. G. Fernandes, N. Kimura, and J. Maki, *Mol. Cryst. Liq. Cryst.* **421**, 243 (2004).
- [20] P. Kahl, P. Baroni, and L. Noirez, *PLoS One* **11**, e0147914 (2016).
- [21] P. Kahl, P. Baroni, and L. Noirez, *Phys. Rev. E* **88**, 050501 (2013).
- [22] INPI, Brazil Patent No. PI 8.801.918-7 (15 April 1998).
- [23] INPI, Brazil Patent No. PI 9.805.500-3 (20 November 1998).
- [24] A. M. Figueiredo Neto, Y. Galerne, A. M. Levelut, and L. Liebert, *J. Phys. (Paris) Lett.* **46**, 499 (1985).
- [25] L. Noirez, *Oil Gas Sci. Technol.* **72**, 10 (2017).
- [26] S. S. Rao, *Mechanical Vibrations*, 3rd ed. (Prentice Hall, Englewood Cliffs, 2011).
- [27] M. Alonso and E. Finn, *Physics* (Addison-Wesley, Reading, 1970).